Int. J. Solids Structures Vol. 27, No. 12, pp. 1499–1514, 1991
Printed in Great Britain.

0020-7683/91 $3.00 + .00

ELASTIC–PLASTIC BEHAVIOUR OF SPHERICAL SHELLS WITH NON-LINEAR HARDENING PROPERTIES

M. M. MEGAHED
Department of Mechanical Design and Production, Cairo University, Giza, Egypt

(*Received* 6 *July* 1989; *in revised form* 4 *May* 1990)

Abstract—This paper considers the elastic–plastic behaviour of thick-walled spheres under internal pressure. Material behaviour is assumed as: $\sigma = Y + A \cdot \varepsilon_p^n$ where Y is an initial yield stress and A and n are material parameters describing the state of hardening. Radial distributions of plastic strains are determined in closed form for four particular values of the exponent n; $n = 1, 1/2, 1/3$ and $1/4$. On the basis of these solutions and a study of practical values of the hardening parameters A and n, a simple approximate relation for plastic strain distribution, which can be used for any value of n, is developed. Validity of the approximate solution is verified and its range of applicability is investigated.

INTRODUCTION

Interest into the elastic–plastic behaviour of thick spherical and cylindrical shells under internal and external pressures, radial thermal gradients and body forces has never ceased (Bland, 1956; Carroll, 1985; Gamer, 1987, 1988; Johnson and Mellor, 1980). Plasticity problems with spherical or cylindrical symmetry can usually be treated analytically, particularly when simplifying assumptions are made regarding material hardening and the reader is referred to Johnson and Mellor (1980) for various interesting assumptions in this area.

Bland (1956) developed analytical solutions for thick-walled tubes made from materials with linear hardening properties and subject to internal and external pressure, and to temperature gradients. Gamer (1988) considered the elastic–plastic behaviour of a thick spherical shell under internal pressure using the same hardening law as the one employed here and developed analytical solutions for two values of the exponent n, viz. $n = 1/2$ and $n = 2$. It is rather strange to take the exponent $n = 2$ since n is usually less than unity for engineering metals. The results reported by Gamer (1988) reveal peculiar stress distributions in the vicinity of the plastic front due to the consideration of hardening parameters A and n which are not representative of common alloys. Gamer's treatment (1988) of the problem is based on Bland's work (1956) which expresses the unknown quantities in terms of the effective stress. However, Gamer's solution (1988) is different from and much simpler than Bland's (1956).

In the present work, the elastic–plastic problem of a thick spherical shell under internal pressure is formulated in a manner which is equivalent to those used by Gamer (1988), Bland (1956) and Bishop *et al.* (1945). However, in the present formulation, the unknown quantities are expressed in terms of effective plastic strain rather than in terms of effective stress.

Practical ranges of the hardening parameters A and n in the hardening law are determined by studying the uniaxial behaviour of about 20 alloys. It is seen that $0 < n < 1$ with $n = 1/3$ being representative of many engineering alloys, as reported by Rees (1987a, b). Thus, the initial objective of the present work is to develop solutions which are applicable to the observed practical values of the hardening exponent n. Hence, closed form expressions are obtained for plastic strain distribution (in terms of plastic front and a hardening function H_c) for four particular values of n, viz. $n = 1, 1/2, 1/3$ and $1/4$. Distributions of radial displacement, tangential and radial stresses can be obtained in closed form for $n = 1$ and $n = 1/2$ but only and in semi-closed form for $n = 1/3$ and $n = 1/4$.

Study of the practical range of parameter A in the hardening law shows that its value is such that the flow stress at plastic strain $= Y/E$ does not exceed two times the initial yield stress Y. Taking this observation into account and carefully inspecting the forms of the analytical distributions of plastic strain at $n = 1$, 1/2, 1/3 and 1/4, enable determination of an approximate general relation for plastic strain distribution which can be used at any value of the exponent n. The accuracy of this approximation is assessed and its ranges of validity are determined.

BASIC EQUATIONS

Consider a thick spherical shell with inner radius $= a$ and outer radius $= b$, subjected to internal pressure P and causing partial plastification. The stress components are σ_θ, σ_θ and σ_r and the total strain components are ε_θ, ε_θ and ε_r. Total strains are decomposed into elastic and plastic components and small strains are assumed. The stress–strain–displacement relations are:

$$\varepsilon_r = \frac{du}{dr} = \frac{1}{E}[\sigma_r - \nu(\sigma_\theta + \sigma_\theta)] + \varepsilon_r^P \tag{1a}$$

$$\varepsilon_\theta = \frac{u}{r} = \frac{1}{E}[\sigma_\theta - \nu(\sigma_r + \sigma_\theta)] + \varepsilon_\theta^P \tag{1b}$$

where u is the radial displacement, r is the generic radius and E and ν are the elastic constants. Compressibility is retained in the elastic range but incompressibility of plastic strains requires that $2\varepsilon_\theta^P + \varepsilon_r^P = 0$. The yielding criterion is the same according to either Tresca or Von Mises; $\bar{\sigma} = \sigma_\theta - \sigma_r$ where $\bar{\sigma}$ is the effective stress. Equations (1a, b) are inverted in order to express stresses in terms of total strains and plastic hoop strain, as follows:

$$\sigma_r = \hat{E}[(1-\nu)\cdot(\varepsilon_r - \varepsilon_r^P) + 2\nu(\varepsilon_\theta - \varepsilon_\theta^P)] \tag{2a}$$

$$\sigma_\theta = \hat{E}[(\varepsilon_\theta - \varepsilon_\theta^P) + \nu(\varepsilon_r - \varepsilon_r^P)], \tag{2b}$$

where $\hat{E} = E/[(1+\nu)\cdot(1-2\nu)]$. Substitution of eqns (2a, b) into the equilibrium condition $d\sigma_r/dr = 2\cdot(\sigma_\theta - \sigma_r)/r$ yields the following differential equation:

$$\frac{d^2u}{dr^2} + \frac{2}{r}\cdot\frac{du}{dr} - \frac{2u}{r^2} = -\frac{2(1-2\nu)}{1-\nu}\left[\frac{d\varepsilon_\theta^P}{dr} + 3\frac{\varepsilon_\theta^P}{r}\right]. \tag{3}$$

Introducing the substitutions:

$$U = u/a \tag{4a}$$

$$X = a/r, \tag{4b}$$

which implies that $X = 1$ at $r = a$ and $X = X_0 = a/b$ at $r = b$, and carrying out the necessary algebraic manipulations yield the solution of eqn (3) as:

$$U = \frac{C}{X} + DX^2 + \frac{1-2\nu}{E}\frac{I}{X} \tag{5a}$$

where

$$I = 2\hat{E}\int_1^X \frac{\varepsilon_\theta^P}{X}\,dX \tag{5b}$$

with

$$\bar{E} = \frac{E}{1-\nu}; \tag{5c}$$

where C and D are integration constants to be determined from the boundary conditions: $\sigma_r = -P$ at $X = 1$ and $\sigma_r = 0$ at $X = X_0$. Upon substitution of the resulting values of C and D into the expressions of displacement, radial and hoop stresses and introducing the further substitution:

$$Z = X^3, \quad Z_0 = X_0^3; \tag{6}$$

the following expressions are obtained:

$$\sigma_r = -P + \frac{1-Z}{1-Z_0}(P-I_0) + I \tag{7a}$$

$$\sigma_\theta = \sigma_r + \frac{3}{2}\cdot\frac{Z}{1-Z_0}(P-I_0) - \bar{E}\cdot\varepsilon_\theta^p \tag{7b}$$

$$U = \frac{1}{E}\left[(1-2\nu)\cdot\sigma_r + \tfrac{1}{2}\cdot(1-\nu)\frac{P-I_0}{1-Z_0}\cdot Z\right]\cdot\frac{1}{\sqrt[3]{Z}} \tag{7c}$$

and the integral I is:

$$I = \tfrac{2}{3}\bar{E}\int_1^Z \frac{\varepsilon_\theta^p}{Z}\,\mathrm{d}Z \tag{7d}$$

and I_0 is the value of I at the plastic front, $Z = \bar{Z}$, i.e.

$$I_0 = \tfrac{2}{3}\bar{E}\int_1^{\bar{Z}} \frac{\varepsilon_\theta^p}{Z}\,\mathrm{d}Z. \tag{7e}$$

Note that $\varepsilon_\theta^p = 0$ and $I = I_0$ throughout the outer elastic zone defined by $Z_0 < Z < \bar{Z}$. At the plastic front, the effective stress $\bar{\sigma} = \sigma_\theta - \sigma_r = Y$ and also $\varepsilon_\theta^p = 0$. Therefore, using eqn (7b) to provide $\bar{\sigma}$, one readily obtains:

$$P - I_0 = \tfrac{2}{3}Y\frac{1-Z_0}{\bar{Z}}. \tag{8}$$

Using eqn (8), the distributions of σ_θ, σ_r and U can be rewritten in simpler forms, as follows:

$$\sigma_r = -P + \tfrac{2}{3}Y\cdot\frac{1-Z}{\bar{Z}} + I \tag{9a}$$

$$\sigma_\theta = \sigma_r + Y\left[\frac{Z}{\bar{Z}} - \hat{\varepsilon}_\theta^p\right] \tag{9b}$$

$$U = \frac{1}{E}\left[(1-2\nu)\sigma_r + (1-\nu)\cdot Y\cdot\frac{Z}{\bar{Z}}\right]\frac{1}{\sqrt[3]{Z}}, \tag{9c}$$

where $\hat{\varepsilon}_\theta^p$ is a normalized plastic hoop strain such that:

$$\bar{\varepsilon}_n^P = \frac{\varepsilon_n^P}{Y/\bar{E}}. \tag{9d}$$

It is obvious from eqn (9b) that the effective stress $\bar{\sigma}$ is simply given by:

$$\bar{\sigma} = Y \cdot \left(\frac{Z}{\bar{Z}} - \bar{\varepsilon}_n^P \right). \tag{10}$$

It is important to notice that eqns (9a, b and c) are valid throughout the entire sphere, with the provision that $I = I_0$ and $\bar{\varepsilon}_n^P = 0$ within the elastic zone. Hence, determination of the entire field of elastic–plastic stresses is reduced to the evaluation of integral I, once the radial distribution of plastic strains is prescribed by means of the hardening law.

A hardening law that has proved to be most relevant in the analysis of small strain plasticity problems is:

$$\bar{\sigma} = Y + A \cdot (\bar{\varepsilon}_P)^n, \tag{11}$$

where A and n are material constants and $\bar{\varepsilon}_P$ is the effective plastic strain. This particular hardening law is preferred to other non-linear hardening representations due to its consistency with observed material behaviour. Note, for example, that the plastic strain is zero and the plastic modulus is infinite at the initial yield, which allows modelling of the observed smooth elastic–plastic transition.

Table 1 lists the values of Y, A and n for a number of engineering alloys as compiled by Megahed (1989). It is clear that the exponent n lies between 0.1 and 0.7, i.e. n is less than unity. In order to characterize the effect of hardening on the flow curve, a hardening function H is defined as the rise in flow stress above the initial yield at a plastic strain equal to Y/E. Hence, the effective stress $\bar{\sigma}$ at $\bar{\varepsilon}_P = Y/E$ is given by:

$$\bar{\sigma} = Y(1 + H) \tag{12a}$$

and H is defined as:

$$H = \frac{A}{Y} \cdot \left(\frac{Y}{E} \right)^n. \tag{12b}$$

Values of H are calculated in Table 1 where it is seen that H is always less than unity. Clearly, perfect plasticity behaviour is obtained when $H = 0$.

Rees (1987a, b) compiled values of A/Y and n for a number of alloys and concluded that $n = 1/3$ can be considered representative of many engineering metals as can be seen

Table 1. Hardening properties of some common alloys (Megahed, 1989)

No.	Material	Y†	A/Y	n	E/Y	H	H_0
1	Ti 7Al 2Cb 1Ta Alloy	500	1.35	0.190	210	0.489	0.521
2	2024-T3 Aluminium	200	2.80	0.206	360	0.883	0.893
3	316 Stainless steel	100	3.65	0.223	1176	0.754	0.813
4	A316 Steel	221	1.67	0.251	936	0.300	0.326
5	A533 PV Steel	330	0.45	0.120	627	0.208	0.216
6	60/40 Brass	140	2.43	0.300	821	0.324	0.359
7	304 Stainless steel	150	5.53	0.445	1333	0.225	0.261
8	99.9% Pure copper	28	8.83	0.373	4167	0.372	0.422
9	6061-O Aluminium	50	16.40	0.629	1280	0.182	0.225
10	Steel S-25C‡	320	3.84	0.710	647	0.039	0.049

† The yield stress Y is in MPa and Poisson's ratio is assumed as 0.3 for all materials.

‡ This material exhibits yield point elongation of about 2% and therefore its hardening curve is represented by $\sigma = Y + A \cdot (\varepsilon_P - \varepsilon_0)^n$ where $\varepsilon_0 = 0.02$.

Table 2. Hardening properties compiled by Rees (1987a, b)

No.	Material	A/Y	n	E/Y†	H	H_s
1	SAE 1020 Steel	4.09	1/3	1000	0.409	0.458
2	14S-T4 Aluminium	3.54	1/3	400	0.480	0.537
3	24S-T4 Aluminium	2.24	1/3	400	0.304	0.340
4	BS-MS1 60/40 Brass	3.49	1/3	1000	0.349	0.390
5	RR 59 Aluminium	2.39	1/3	800	0.257	0.288
6	Ti 50A Titanium	3.72	0.450	400	0.251	0.292
7	EN 32B Steel	1.30	0.17	1000	0.402	0.425
8	E1A Aluminium	15.18	0.562	800	0.355	0.428
9	2014 T4 Aluminium	2.22	0.300	400	0.368	0.407
10	EN 24 Steel	6.79	0.738	1000	0.042	0.053
11	EN 25 Steel	3.29	0.664	1000	0.034	0.042

† Poisson's ratio is assumed as 0.3 for all materials and reasonable approximae values are assumed for E/Y.

from Table 2. Again, values of the hardening function H are determined and found to be always less than unity. It is worth noting that quite small values of H can be obtained at relatively large values of the hardening exponent n coupled with small values of A/Y. This can be clearly seen from the data of 6061-O aluminium, EN 24 and EN 25 steels given in Table 2.

ANALYTICAL SOLUTIONS FOR PLASTIC HOOP STRAIN

The effective plastic strain in the sphere problem is $\bar{\varepsilon}_p = 2\varepsilon_\theta^p$ and hence the hardening law can be rewritten in terms of the normalized plastic hoop strain, $\tilde{\varepsilon}_\theta^p$, as:

$$\bar{\sigma} = Y[1 + H_s(\tilde{\varepsilon}_\theta^p)^n], \tag{13a}$$

where H_s represents the hardening function for the sphere problem and defined as:

$$H_s = \frac{A}{Y} \cdot \left(\frac{2Y}{\bar{E}}\right)^n. \tag{13b}$$

Values of H_s are determined for the material constants listed in Tables 1 and 2 and found to be less than unity. A comparison between the expressions for effective stress provided by eqns (10) and (13a) yields the following non-linear equation in $\tilde{\varepsilon}_\theta^p$:

$$H_s(\tilde{\varepsilon}_\theta^p)^n + \tilde{\varepsilon}_\theta^p - \left(\frac{Z}{\bar{Z}} - 1\right) = 0. \tag{14}$$

One of the real roots of eqn (14) should provide the radial distribution of plastic hoop strain. The roots cannot be determined analytically except for some particular values of n. Analytical solutions are provided here for $n = 1$, 1/2, 1/3 and 1/4.

For $n = 1$, eqn (14) is linear and $\tilde{\varepsilon}_\theta^p$ is given by:

$$\tilde{\varepsilon}_\theta^p = \frac{1}{1 + H_s}\left(\frac{Z}{\bar{Z}} - 1\right), \tag{15a}$$

where $H_s = (A/Y) \cdot (2Y/\bar{E}) = 2A/\bar{E}$ is the hardening function at $n = 1$. The integral I is evaluated as:

$$I = \frac{2Y}{3(1+H_s)}\left[\frac{Z-1}{\bar{Z}} - \ln Z\right]. \tag{15b}$$

The value of I_0 is determined by setting $Z = \bar{Z}$ in eqn (15b) and by substitution into eqn (8); the plastic front $\bar{Z}$ is related non-linearly to the applied pressure P. All the necessary information has now been established to determine stresses and displacement, according to eqns (9a, b and c).

For $n = 1/2$, eqn (14) is quadratic and only one of its roots satisfies the prerequisite, $\bar{\varepsilon}_\theta^p = 0$, at the plastic front. This root is:

$$\bar{\varepsilon}_\theta^p = \frac{Z}{\bar{Z}} - 1 + \tfrac{1}{2}H_s^2 - H_s\sqrt{\frac{Z}{\bar{Z}} - 1 + \tfrac{1}{4}H_s^2}, \tag{16a}$$

where $H_s = (A/Y)\cdot\sqrt{2Y/\bar{E}}$ is the hardening function for $n = 1/2$. The integral I can be evaluated analytically in this case also, as follows:

$$I = \frac{2Y}{3}\left[\frac{Z-1}{\bar{Z}} - (1-\tfrac{1}{2}H_s^2)\ln Z - 2H_s\left(\sqrt{\frac{Z}{\bar{Z}} - 1 + \tfrac{1}{4}H_s^2} - \sqrt{\frac{1}{\bar{Z}} - 1 + \tfrac{1}{4}H_s^2}\right)\right.$$
$$\left. + 2H_s\cdot\sqrt{1-\tfrac{1}{4}H_s^2}\cdot\left(\arccos\sqrt{\frac{\bar{Z}}{Z}\left(1-\frac{H_s^2}{4}\right)} - \arccos\sqrt{\bar{Z}\left(1-\frac{H_s^2}{4}\right)}\right)\right]. \tag{16b}$$

The value of $I_0 = I(\bar{Z})$ and eqn (8) is used to provide the non-linear relation between pressure and plastic front.

For $n = 1/3$, eqn (14) becomes a cubic equation taking the following form:

$$(\bar{\varepsilon}_\theta^p)^3 - 3\left(\frac{Z}{\bar{Z}} - 1\right)\cdot(\bar{\varepsilon}_\theta^p)^2 + \left[3\left(\frac{Z}{\bar{Z}} - 1\right)^2 + H_s^3\right]\cdot\bar{\varepsilon}_\theta^p - \left(\frac{Z}{\bar{Z}} - 1\right)^3 = 0, \tag{17a}$$

where $H_s = (A/Y)\cdot(2Y/\bar{E})^{1/3}$ is the hardening function at $n = 1/3$. The discriminant of eqn (17a) is

$$\frac{H_s^2}{2}\sqrt{\frac{4H_s^3}{27} + \left(\frac{Z}{\bar{Z}} - 1\right)^2},$$

which is clearly greater than zero, indicating one real root and two imaginary roots. The real root provides the distribution of $\bar{\varepsilon}_\theta^p$ as:

$$\bar{\varepsilon}_\theta^p = \frac{Z}{\bar{Z}} - 1 + H_s\cdot\left[\frac{1}{2}\sqrt{\frac{4H_s^3}{27} + \left(\frac{Z}{\bar{Z}} - 1\right)^2} - \frac{1}{2}\left(\frac{Z}{\bar{Z}} - 1\right)\right]^{1/3}$$
$$- H_s\cdot\left[\frac{1}{2}\sqrt{\frac{4H_s^3}{27} + \left(\frac{Z}{\bar{Z}} - 1\right)^2} + \frac{1}{2}\left(\frac{Z}{\bar{Z}} - 1\right)\right]^{1/3}. \tag{17b}$$

The analytical evaluation of integral I is rather difficult in this case and we have to resort to numerical integration.

In the case of $n = 1/4$, eqn (14) becomes a quartic equation taking the following form:

$$[\bar{\varepsilon}_\theta^p]^4 - 4\left(\frac{Z}{\bar{Z}} - 1\right)[\bar{\varepsilon}_\theta^p]^3 + 6\left(\frac{Z}{\bar{Z}} - 1\right)^2[\bar{\varepsilon}_\theta^p]^2 - \left[4\left(\frac{Z}{\bar{Z}} - 1\right)^3 + H_s^3\right]\cdot\bar{\varepsilon}_\theta^p + \left(\frac{Z}{\bar{Z}} - 1\right)^4 = 0, \tag{18a}$$

where $H = (A/Y)\cdot(2Y/\bar{E})^{1/4}$ is the hardening function corresponding to $n = 1/4$. It can be shown that eqn (18a) possesses two real roots and two imaginary roots with only one of its real roots satisfying the prerequisite that $\bar{\varepsilon}_\theta^p = 0$ at the plastic front. This root is given by:

$$\bar{\varepsilon}_\theta^p = \frac{Z}{\bar{Z}} - 1 + K\left[1 - \sqrt{\frac{H_s^4}{4K^3} - 1}\right]. \tag{18b}$$

where

$$K^2 = \tfrac{1}{2}H_s^2\cdot\left[\sqrt{\left(\frac{Z/\bar{Z}-1}{3}\right)^3 + \left(\frac{H_s}{4}\right)^4} + \left(\frac{H_s}{4}\right)^2\right]^{1/3} - \tfrac{1}{2}H_s^2\cdot\left[\sqrt{\left(\frac{Z/\bar{Z}-1}{3}\right)^3 + \left(\frac{H_s}{4}\right)^4} - \left(\frac{H_s}{4}\right)^2\right]^{1/3}. \tag{18c}$$

Similar to the case of $n = 1/3$, the analytical evaluation of integral I is difficult if not impossible in this case and has to be determined numerically.

It is worth noting that the well-known perfect plasticity solution is retrievable from any of the above solutions by letting the hardening function $H_s = 0$. This serves as verification of the above results. It is worth noting that for a given plastic front, the distributions of σ_r, σ_θ and u can be determined in closed form for $n = 1$ and $n = 1/2$, only because integral I is evaluated analytically in these cases. For $n = 1/3$ and $n = 1/4$, integral I cannot be evaluated analytically.

The above solutions can be used to study the influence of hardening (as expressed by H_s and n) on the distribution of elastic-plastic stresses induced in the sphere. A spherical shell, with $b/a = 2$ and elastic constants $E/Y = 1000$ and $\nu = 0.3$, is considered. First, the shell is assumed to be fully plasticized, i.e. $\bar{r} = b = 2a$. Radial distributions of σ_r and σ_θ are shown in Figs 1a, b, c and d for $n = 1$, 1/2, 1/3 and 1/4, respectively. For each value of n, stresses are determined at six values of H_s viz. $H_s = 0$, 0.2, 0.4, 0.6, 0.8 and 1. It is seen that for a given value of n, tangential stress increases and radial stress decreases as a result of increasing the hardening function, H_s. The pressure carrying capacity (σ_r at $r = a$) is substantially increased as H_s increases, particularly at large values of the exponent n.

Figures 2a, b, c and d present a similar set of results for the same shell as above when partially plasticized up to $\bar{r} = 1.6a$. The influences of H_s and n are similar to those observed in Fig. 1, except that the pressure carrying capacity does not seem to be affected by n for a given value of H_s. Figure 3 summarizes the influence of H_s and n on σ_θ and σ_r at $r = a$ for the fully plasticized shell (Fig. 3a) and the partially plasticized shell (Fig. 3b).

AN APPROXIMATE GENERAL SOLUTION

Careful inspection of the analytical solutions obtained earlier for $\bar{\varepsilon}_\theta^p$ at the four values of n enable the development of a general approximate solution that can be used at any value of n. The approach here is based upon the observation that practical values of H_s are always less than unity and often less than 0.5 for many engineering alloys, as can be seen from Tables 1 and 2.

Consider firstly, eqn (16a) which provides the exact radial distribution of $\bar{\varepsilon}_\theta^p$ for $n = 1/2$. Since $H_s < 1$, then fractions of H_s^2 appearing in eqn (16a) can be considered small enough in comparison with $(Z/\bar{Z}-1)$, particularly at radii far enough from the plastic front. Thus, neglecting $H_s^2/2$ and $H_s^2/4$ yields the following approximate expression for $\bar{\varepsilon}_\theta^p$ at $n = 1/2$:

$$\bar{\varepsilon}_\theta^p = (Z/\bar{Z}-1) - H_s\cdot(Z/\bar{Z}-1)^{1/2}. \tag{19a}$$

Consider eqn (17b) which provides the exact distribution of $\bar{\varepsilon}_\theta^p$ for $n = 1/3$. Neglecting the

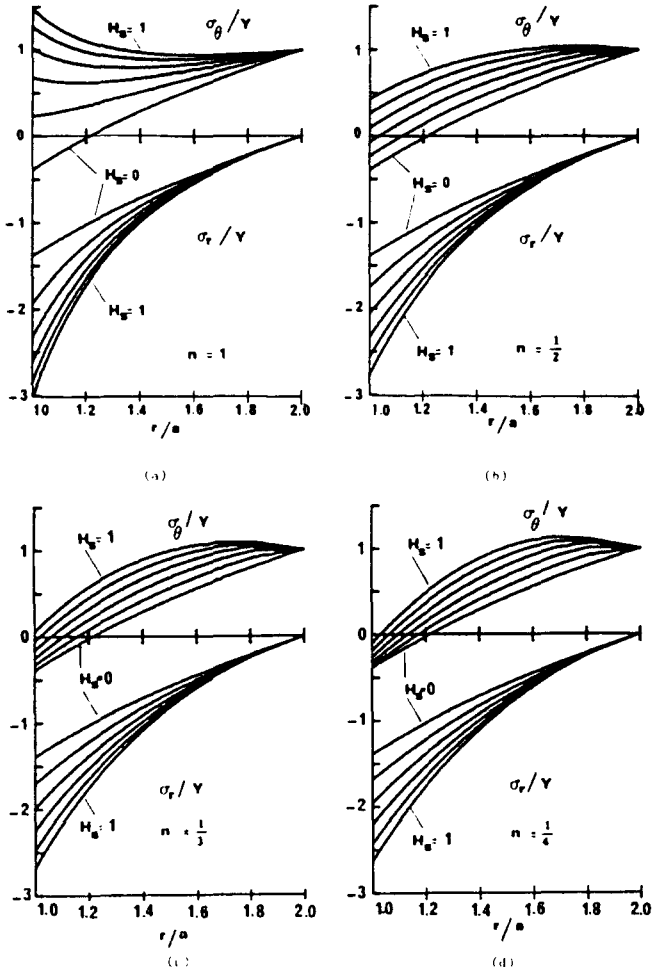

Fig. 1. Distributions of radial and tangential stresses in a fully plasticized shell ($\bar{r} = 2a$) at various values of H_s and n: (a) $n = 1$, (b) $n = 1/2$, (c) $n = 1/3$, and (d) $n = 1/4$.

term $4H_s^3/27$ in comparison with $(Z/\bar{Z}-1)^2$ yields the following approximate expression for $\bar{\varepsilon}_\theta^p$ at $n = 1/3$:

$$\bar{\varepsilon}_\theta^p = (Z/\bar{Z}-1) - H_s \cdot (Z/\bar{Z}-1)^{1/3}. \tag{19b}$$

Consider now, eqns (18b and c) which provide the exact distribution of $\bar{\varepsilon}_\theta^p$ for $n = 1/4$. In eqn (18c), neglecting $(H_s/4)^4$ with respect to $((Z/\bar{Z}-1)/3)^3$ in the square root term yields:

$$K^2 = \tfrac{1}{2}H_s^2\left(\frac{\psi}{3}\right)^{1/2}\left\{\left[1+\frac{(H_s/4)^2}{(\psi/3)^{3/2}}\right]^{1/3} - \left[1-\frac{(H_s/4)^2}{(\psi/3)^{3/2}}\right]^{1/3}\right\}, \tag{19c}$$

where $(Z/\bar{Z}-1)$ is denoted by ψ. Since $(H_s/4)^2/(\psi/3)^{3/2}$ is much less than unity at radii far enough from the plastic front, expansion of the cubic root terms by $(1+x)^m \simeq 1+m\cdot x$ for $x \ll 1$ and simplifying yield:

$$K^2 = \frac{(H_s^2/4)^2}{Z/\bar{Z}-1}, \quad \frac{H_s^4}{4K^3} = \frac{(Z/\bar{Z}-1)^{1/2}}{H_s^2/4}. \tag{19d}$$

Substitution into eqn (18b) gives:

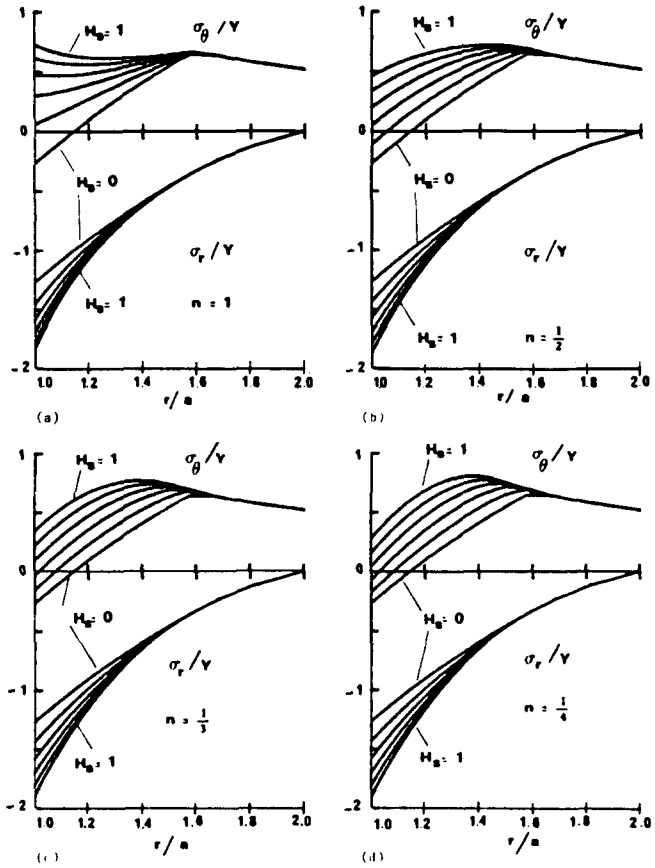

Fig. 2. Distributions of radial and tangential stresses in a partially plasticized shell ($\bar{r} = 1.6a$) at various values of H_s and n: (a) $n = 1$, (b) $n = 1/2$, (c) $n = 1/3$, and (d) $n = 1/4$.

$$\bar{\varepsilon}_\theta^p = (Z/\bar{Z}-1) + \frac{H_s}{(Z/\bar{Z}-1)^{1/2}}\left[\frac{H_s}{4} - \sqrt{(Z/\bar{Z}-1)^{1/2} - (H_s/4)^2}\right]. \tag{19e}$$

Neglecting $(H_s/4)^2$ with respect to $(Z/\bar{Z}-1)^{1/2}$ in the square root term and also neglecting $H_s/4$ with respect to $(Z/\bar{Z}-1)^{3/4}$ in the resulting expression yield the final approximate relation as:

$$\bar{\varepsilon}_\theta^p = (Z/\bar{Z}-1) - H_s(Z/\bar{Z}-1)^{1/4}. \tag{19f}$$

It is worth noting that eqn (15a), which gives the exact distribution of $\bar{\varepsilon}_\theta^p$ for $n = 1$, can also be rewritten as:

$$\bar{\varepsilon}_\theta^p = (Z/\bar{Z}-1) - H_s(Z/\bar{Z}-1), \tag{19g}$$

provided that $H_s \ll 1$ such that $1/(1+H_s) \simeq 1 - H_s$. Therefore, at relatively large values of H_s, the approximation provided by eqn (19g) will be poor at $n = 1$.

Inspection of eqns (19a, b, f and g) reveals that a simple general pattern is emerging for approximate description of $\bar{\varepsilon}_\theta^p$ at any value of the exponent n, viz.

$$\bar{\varepsilon}_\theta^p = (Z/\bar{Z}-1) - H_s \cdot (Z/\bar{Z}-1)^n. \tag{20}$$

A number of important points are worth noting at this stage:

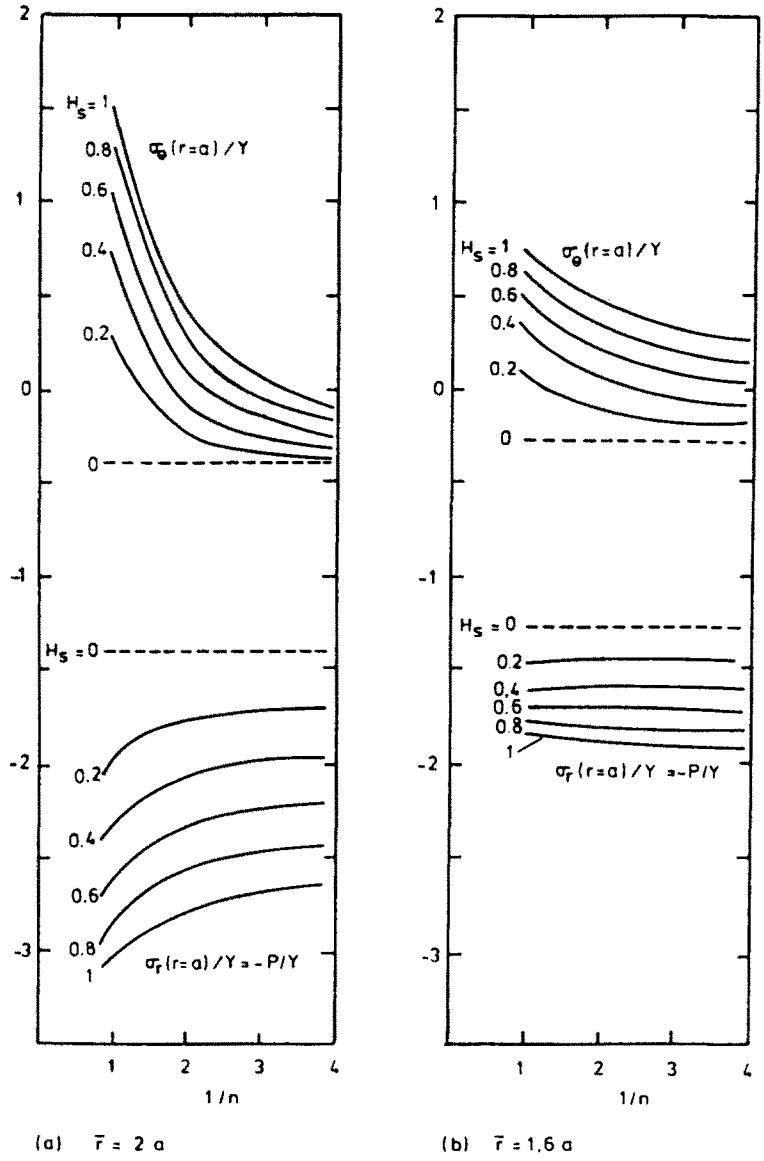

Fig. 3. Influence of H_s and n on stresses at the inner radius of the shell ($b/a = 2$, $E/Y = 1000$, $\nu = 0.3$). (a) Fully plasticized and (b) partially plasticized.

(1) The first term in eqn (20) is the well-known perfect plasticity solution for $\dot{\varepsilon}_\theta^p$. Therefore, the second term represents a quantification of the inhibition of plastic strain development due to hardening.

(2) Neglecting fractions of positive powers of H_s in comparison with positive powers of $(Z/\bar{Z}-1)$ is quite valid at radii located too far from the plastic front. However, at radii close to the plastic front, $(Z/\bar{Z}-1)$ also becomes very small and the above approximation is not strictly valid. The resulting errors in $\dot{\varepsilon}_\theta^p$ are not likely to be great since $\dot{\varepsilon}_\theta^p$ itself is quite small in the vicinity of the plastic front.

(3) Inspection of eqn (20) indicates that $\dot{\varepsilon}_\theta^p = 0$ at two values of Z; at $Z = \bar{Z}$, i.e. at the plastic front and also at $Z = Z^*$ where

$$Z^* = \bar{Z}[1 + H_s^{1/(1-n)}]. \tag{21}$$

This implies that $\dot{\varepsilon}_\theta^p$ is negative in the zone bounded by $\bar{Z} < Z < Z^*$. Since negative

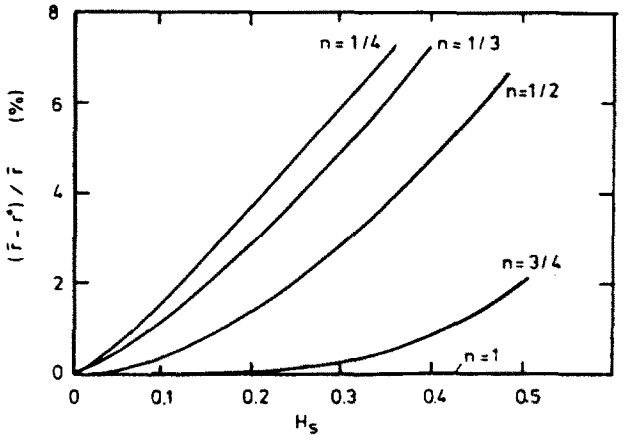

Fig. 4. Variation of $(\bar{r}-r^*)/\bar{r}$ (%) with H_s and n.

plastic strain cannot be permitted, $\bar{\varepsilon}_\theta^p$ will be taken as zero in the zone bounded by $\bar{Z} < Z < Z^*$. Therefore, a clearer statement of the approximate solution will be:

$$\bar{\varepsilon}_\theta^p = (Z/\bar{Z}-1) - H_s(Z/\bar{Z}-1)^n \quad \text{for} \quad Z^* < Z < 1 \tag{22a}$$

$$\bar{\varepsilon}_\theta^p = 0 \quad \text{for} \quad \bar{Z} < Z < Z^*. \tag{22b}$$

The ratio $\bar{Z}/Z^*$ can be very close to unity depending on H_s and n. Figure 4 shows the variation of the relative difference between $\bar{r}$ and r^* (corresponding to $\bar{Z}$ and Z^*, respectively), with H_s at various values of n. Generally, the relative error is quite small with its value becoming larger as H_s increases and n decreases simultaneously. At $n = 1$, note that $(\bar{r}-r^*)/\bar{r} = 0$, whatever the value of H_s. Since the approximate solution has been shown to be poor at $n = 1$ when relatively large values of H_s are encountered [see eqn (19g)], it appears that the proximity between r^* and $\bar{r}$ cannot be used alone as a sole measure of the accuracy of the proposed approximate solution.

(4) Although eqn (20) is derived here, starting from exact solutions at some particular values of the exponent n, it is believed that the above approximation is valid for any value of n as it probably amounts to a first approximation to the solution of the non-linear relation provided by eqn (14). A detailed comparison between exact and approximate solution is presented in the following.

COMPARISON BETWEEN EXACT AND APPROXIMATE SOLUTIONS

A comparison between the exact solutions developed earlier and the approximate solution is illustrated for a tube with $b/a = 2$, $\bar{r}/a = 2$, $E/Y = 1000$ and $\nu = 0.3$. A representative value of $H_s = 0.3$ is adopted and the comparison is made for three different values of the exponent n; $n = 1/2$, $1/3$ and $1/4$ as shown in Figs 5a, b and c, respectively. In general, agreement between exact and approximate distributions of σ_θ, σ_r and $\bar{\varepsilon}_\theta^p$ is quite satisfactory. The maximum discrepancy in σ_θ and $\bar{\varepsilon}_\theta^p$ is confined to the vicinity of the plastic front while the maximum discrepancy in σ_r is at the inner radius of the sphere.

An overall picture of the performance of the approximate solution is provided by the results given in Table 3, which compares the pressure carrying capacity as predicted by exact and approximate solutions for a fully plasticized shell ($b/a = 2$, $E/Y = 1000$, $\nu = 0.3$) at various values of H_s and n. The pressure predicted by the approximate solution exceeds the exact pressure slightly. Figure 6a shows the percentage error in pressure against H_s at $n = 1$, $1/2$, $1/3$ and $1/4$. The errors in approximate pressure are seen not to be excessive, except when H_s and n become relatively large. Notice in particular, the poor performance of the approximate solution at $n = 1$ when H_s exceeds about 0.2.

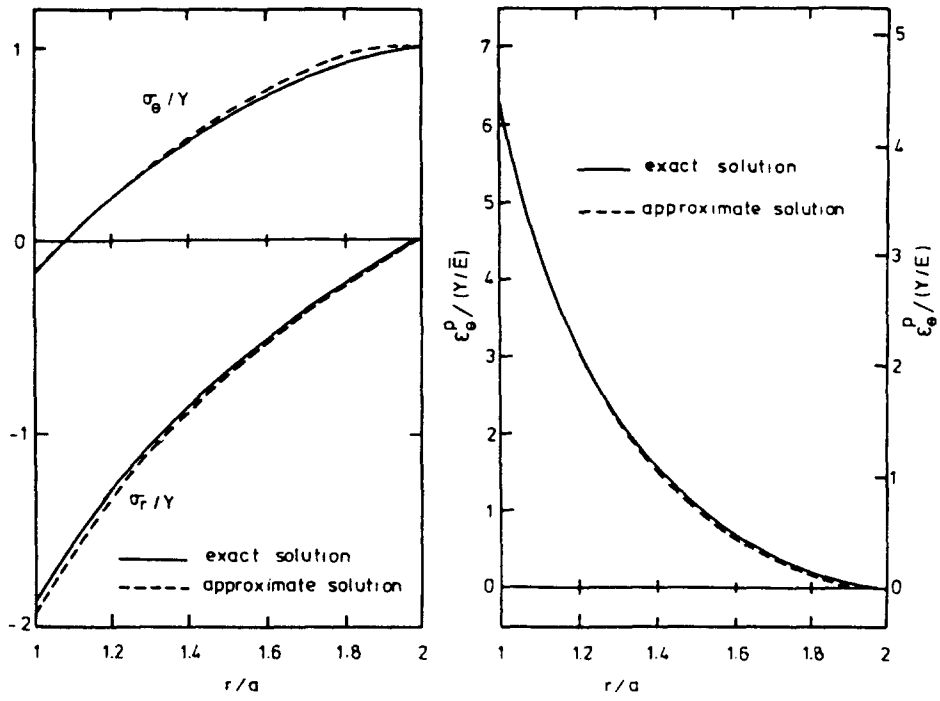

Fig. 5a. Comparison between exact and approximate solutions for a sphere with $b/a = 2$, $\bar{r}/a = 2$ and material parameters: $H_s = 0.3$, $n = 1/2$, $E/Y = 1000$ and $\nu = 0.3$.

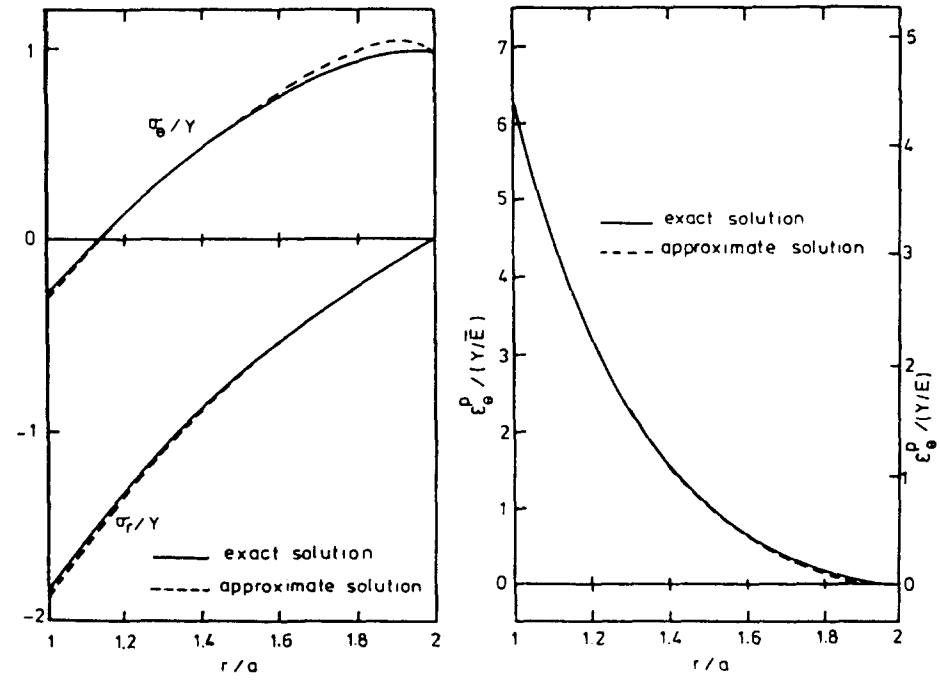

Fig. 5b. Comparison between exact and approximate solutions for a sphere with $b/a = 2$, $\bar{r}/a = 2$ and material properties: $H_s = 0.3$, $n = 1/3$, $E/Y = 1000$ and $\nu = 0.3$.

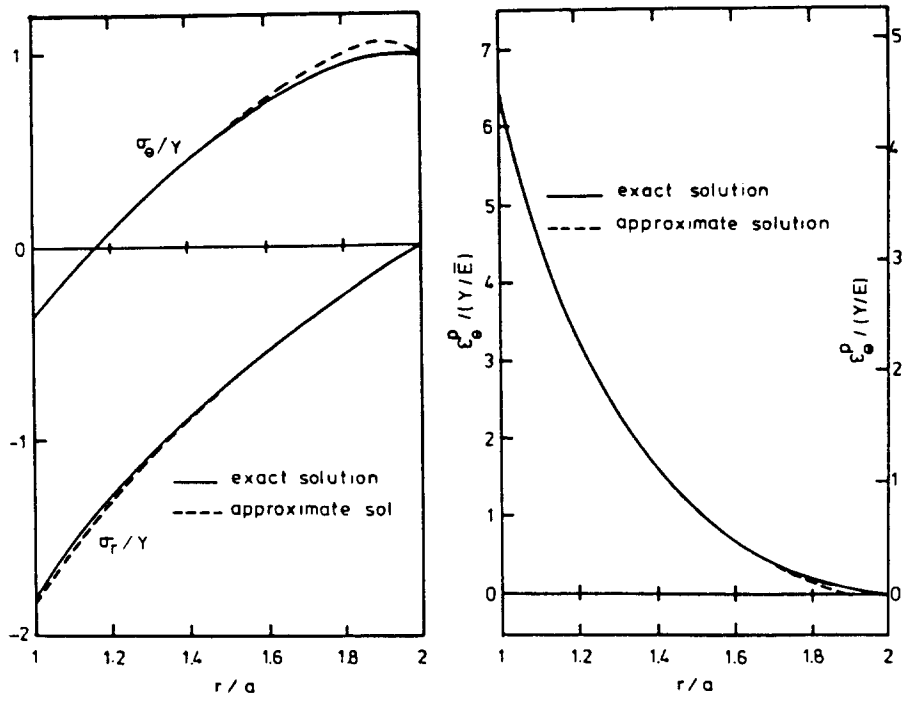

Fig. 5c. Comparison between exact and approximate solutions for a sphere with $b/a = 2$, $\bar{r}/a = 2$ and material properties: $H_s = 0.3$, $n = 1/4$, $E/Y = 1000$ and $\nu = 0.3$.

Table 3. Approximate/exact pressure (P/Y) for a fully plasticized sphere with $b/a = 2$, $E/Y = 1000$ and $\nu = 0.3$

n	$H_s = 0.1$	0.2	0.3	0.4	0.5
1/4	1.543/1.539	1.698/1.685	1.850/1.824	1.999/1.955	2.144/2.081
1/3	1.553/1.548	1.718/1.702	1.882/1.847	2.043/1.984	2.201/2.114
1/2	1.578/1.571	1.769/1.743	1.960/1.903	2.150/2.053	2.337/2.193
1	1.715/1.685	2.043/1.933	2.371/2.143	2.698/2.326	3.027/2.480

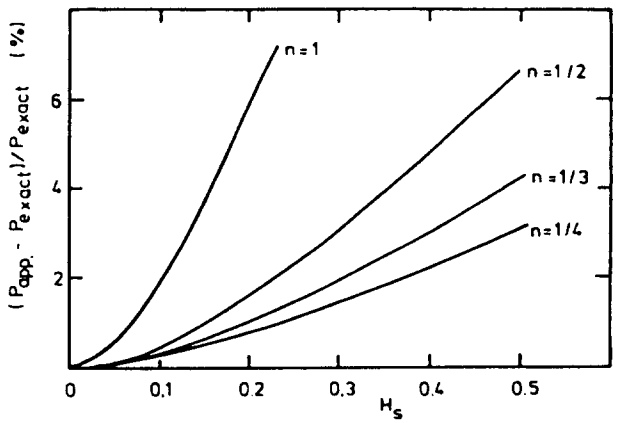

Fig. 6a. Variation of percentage error in pressure carrying capacities with H_s and n.

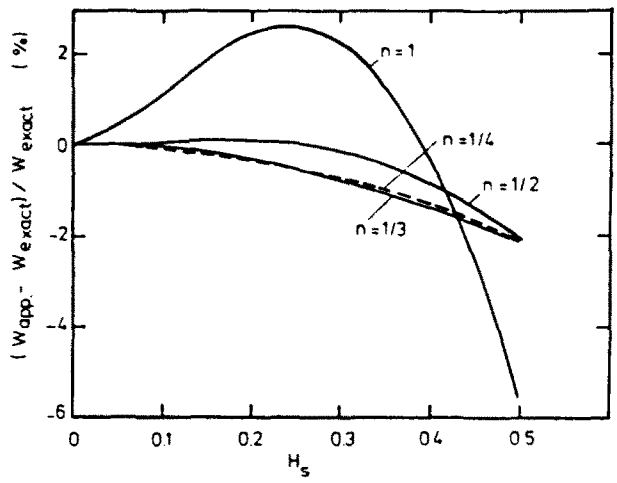

Fig. 6b. Variation of percentage error in work ratios W_{wh}/W_{pp} with H_s and n.

Table 4. Approximate/exact work ratio W_{wh}/W_{pp} for a fully plasticized shell with $b/a = 2$, $E/Y = 1000$ and $\nu = 0.3$

n	$H_s = 0.1$	0.2	0.3	0.4	0.5
1/4	1.051/1.051	1.088/1.093	1.116/1.124	1.133 1.148	1.142/1.165
1/3	1.060/1.061	1.106/1.109	1.138/1.147	1.158/1.174	1.168/1.193
1/2	1.082/1.081	1.146/1.144	1.189/1.191	1.214 1.224	1.221/1.246
1	1.176/1.163	1.293/1.261	1.347/1.316	1.340 1.343	1.271/1.351

Another plausible measure of the adequacy of the approximate solution is the ratio between total internal dissipation of work in a sphere made from a work hardening material W_{wh} and work dissipated in a similar sphere made from a perfectly plastic material W_{pp}. Table 4 gives the values of this work ratio as predicted by exact and approximate solutions for a fully plasticized sphere ($b/a = 2$, $E/Y = 1000$ and $\nu = 0.3$) at various values of H_s and the four values of the exponent n ($n = 1$, 1/2, 1/3 and 1/4). The percentage errors between exact and approximate values of W_{wh}/W_{pp} are shown in Fig. 6b against H_s at the different values of n. The errors in total dissipated work are quite small for $n = 1/2$, 1/3 and 1/4 but are highly dependent on H_s for $n = 1$.

The above analysis shows that the approximate solution can be used with confidence for values of H_s less than about 0.5 and values of the exponent n not close to unity. Naturally, these limitations can be relaxed depending on the accuracy required. Fortunately, values of H_s and n for many engineering metals lie within the above limits, as can be seen from the data of Tables 1 and 2. Adequacy of the approximate solution is checked above for a fully plasticized shell. For a partially plasticized shell, the accuracy of the approximation will depend upon the position of the plastic front. Clearly, if $(Z/\bar{Z} - 1)$ is relatively small because the plastic front is too close to the inner radius of the shell, the resulting errors in the approximate solution may not be tolerated. For these cases of limited plasticity, one has to rely on the exact solutions provided here for a wide range of the exponent n.

Finally, two examples of the application of the approximate solution to actual materials are shown in Fig. 7 for partially plasticized spheres ($\bar{r}/a = 1.8$), where actual material data of 304 stainless steel and 6061-O aluminium are used.

DISCUSSION AND CONCLUSIONS

Exact and approximate distributions of plastic strain in similar elastic–plastic problems can be obtained in a manner analogous to that presented here. An example of such problems is reported by Megahed (1989) for a thick tube under internal pressure. Loading conditions such as external pressure, radial thermal gradient and centrifugal forces can be included in

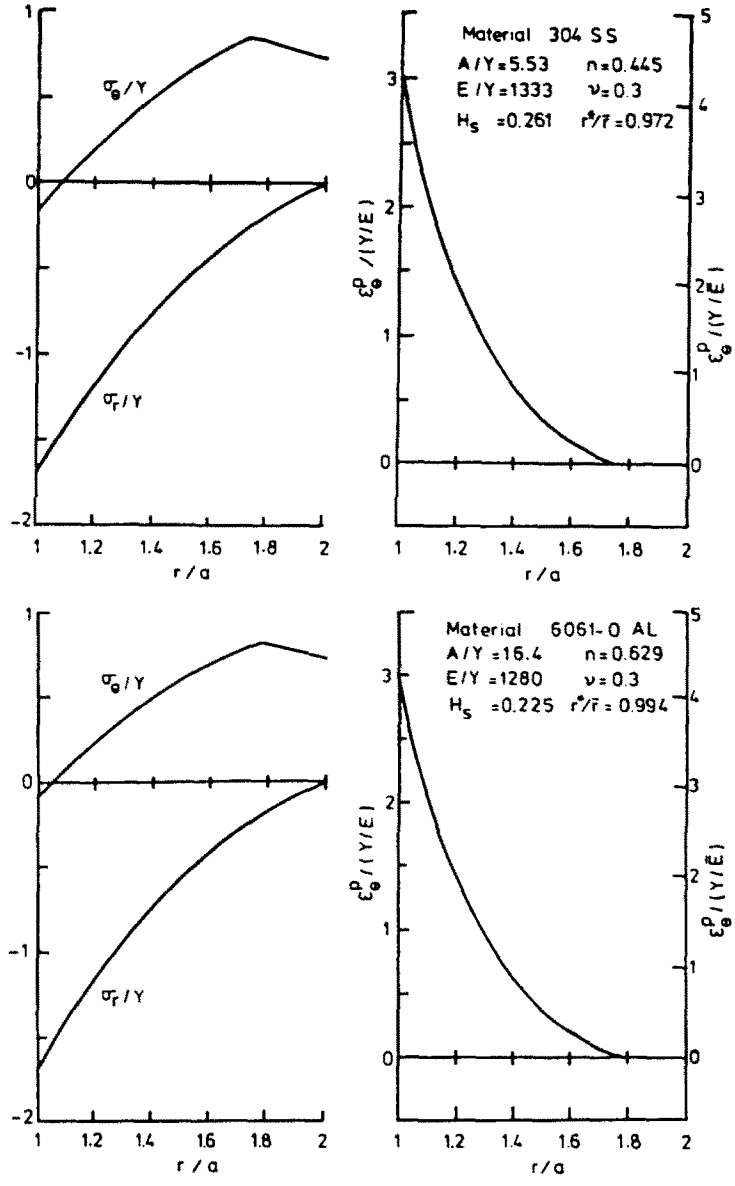

Fig. 7. Examples of the approximate distributions of stresses and plastic strain in partially plasticized shells ($\bar{r}/a$ = 1.8) and using the actual material properties of 304 SS and 6061-O aluminium.

the analysis. Future work may also include the elastic-plastic unloading behaviour. This will enable determination of realistic etimates of residual stresses which are usually determined on the basis of isotropic hardening, which ignores the softening behaviour during reverse loading as manifested by the Bauschinger effect.

The general approximate solution developed here provides a quick and reliable estimate of elastic-plastic stresses and displacement for spheres made from the most common engineering metals. It is worth noting that the development of the approximate solution could not have been possible without the exact solutions developed earlier in the paper.

REFERENCES

Bishop, R. F., Hill, R. and Mott, F. R. S. (1945). The theory of indentation and hardness tests. *Proc. Phys. Soc.* 57, 147–159.

Bland, D. R. (1956). Elastoplastic thick walled tubes of work hardening material subject to internal and external pressure and to temperature gradients. *J. Mech. Phys. Solids* 4, 200–229.

Carroll, M. M. (1985). Radial expansion of hollow spheres of elastic plastic hardening materials. *Int. J. Solids Structures* **21**, 645–670.

Gamer, U. (1987). The shrink fit with elastic plastic hub exhibiting constant yield stress followed by hardening. *Int. J. Solids Structures* **23**, 1219–1224.

Gamer, U. (1988). The expansion of elastic plastic spherical shell with non-linear hardening. *Int. J. Mech. Sci.* **30**, 415–426.

Johnson, W. and Mellor, P. B. (1980). *Engineering Plasticity*, Chapter 9. Van Nostrand Reinhold, London.

Megahed, M. M. (1990). Elastic plastic behaviour of a thick walled tube with general non-linear hardening properties. *Int. J. Mech. Sci.* **32**, 551–563.

Rees, D. W. A. (1987a). An experimental appraisal of equi-plastic strain multi-surface hardening model. *Acta Mech.* **70**, 193–219.

Rees, D. W. A. (1987b). Application of classical plasticity theory to non-radial loading paths. *Proc. Royal Society—London* **A410**, 443–475.